

Article

Corrosion Inhibition of Low-Carbon Steel by Hydrophobic Organosilicon Dispersions

Yuri Makarychev, Natalia Gladkikh *, Ivan Arkhipushkin and Yuri Kuznetsov

Frumkin Institute of Physical Chemistry and Electrochemistry, Russian Academy of Sciences, 119071 Moscow, Russia; makarychev-1949@mail.ru (Y.M.); arhi90@mail.ru (I.A.); yukuzn@gmail.com (Y.K.)

* Correspondence: fuchsia32@bk.ru

Abstract: This article proposes a method for obtaining stable hydrophobic inhibitor dispersions, where the micelle core contains a hydrophobic solvent, a corrosion inhibitor and an organosilane. Such compositions can be used as polymer-type corrosion inhibitors for low-carbon steel. Using electrochemical methods, corrosion tests and X-ray photoelectron spectroscopy, features of the formation of polymeric layers of hydrophobic organosilicon dispersions were studied.

Keywords: organosilanes; inhibitor dispersions; corrosion resistance



Citation: Makarychev, Y.; Gladkikh, N.; Arkhipushkin, I.; Kuznetsov, Y. Corrosion Inhibition of Low-Carbon Steel by Hydrophobic Organosilicon Dispersions. *Metals* **2021**, *11*, 1269. <https://doi.org/10.3390/met11081269>

Academic Editor: Anna H. Kaksonen

Received: 19 July 2021

Accepted: 9 August 2021

Published: 11 August 2021

Publisher's Note: MDPI stays neutral with regard to jurisdictional claims in published maps and institutional affiliations.



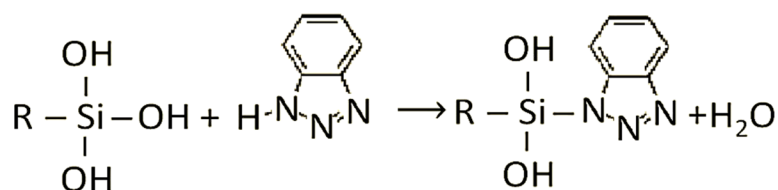
Copyright: © 2021 by the authors. Licensee MDPI, Basel, Switzerland. This article is an open access article distributed under the terms and conditions of the Creative Commons Attribution (CC BY) license (<https://creativecommons.org/licenses/by/4.0/>).

1. Introduction

In recent years, for corrosion prevention, new methods of metal surface modification have been used, based on the use of environmentally friendly substances, which include organosilicon compounds, in particular, organosilanes [1–5]. For these purposes, numerous studies are being carried out on the use of organosilanes as corrosion inhibitors for various metallic materials, including low-carbon steels [5–13]. Organosilanes are environmentally friendly substances that can stop the corrosive dissolution of a metal. Organosilanes do not occur naturally; they are mainly synthesized from silicon dioxide. The general formula is $R_nSi(OEt)_{4-n}$, where R is an organofunctional group, and OEt is a hydrolyzable group (methoxy, ethoxy or acetoxy). In the presence of water, the hydrolyzable R group tends to form an active silanol group ($\equiv Si-OH$), which is capable of interacting with a hydroxyl group on the metal surface ($\equiv Si-O-Me$), and subsequent polycondensation leads to the formation of siloxane groups ($\equiv Si-O-Si \equiv$) [11–13]. In addition to organosilanes, corrosion inhibitors are used to reduce the corrosivity of media. A large number of effective corrosion inhibitors in various environments are known today. Oxidative corrosion inhibitors (chromates, molybdates, tungstates, etc.) have good protective properties against many structural metals in a wide pH range, but chromates are toxic, and their use is excluded [12,14]. Tungstates and molybdates have a chemical structure similar to chromates; however, they are not as effective and have a high cost, which sharply limits their application. Inhibitors of the oxidative type can be replaced with inhibitors of the adsorption type. As a result of adsorption of the inhibitor on the metal surface, protective layers are formed—poorly soluble complex compounds. Adsorption inhibitors are cheaper and more accessible than oxidative inhibitors, but they are not always functional for the protection of metals [15–17]. It is advisable to use an inhibitor composition that would consist of corrosion inhibitor molecules and an organosilane.

In our previous studies, it was shown that inhibitor compositions which are a mixture of organosilane vinyltrimethoxysilane (VS) and an adsorption-type corrosion inhibitor (1,2,3-benzotriazole (BTA)) are capable of forming polymer-like layers with high protective properties on the metal surface against local (pitting) and general corrosion. Moreover, the inhibition effectiveness of compositions is much higher than that of each inhibitor separately [12,13]. The synergism of a composition arises from the presence of BTA, which is capable of forming poorly soluble protective compounds on a metal surface [18–30] and

is also a copolymer in the polycondensation reaction on the metal surface according to Scheme 1.



Scheme 1. Polycondensation reaction of silanol and benzotriazole.

However, the formation of polymer-like structures with the participation of an organosilane and a corrosion inhibitor occurs not only on the surface of metals but also in the bulk of the solution, which makes it difficult to store these compositions and use them for a long time, for example, when protecting cooling systems, or when using water-borne paints. It is possible to prevent the polymerization of organosilanes in the volume of aqueous solutions if they are used in the form of inhibitor dispersions (IDs) [31]. In this case, the micelle core is a solution of an inhibitor composition based on a hydrophobic solvent. The aim of this study was to develop inhibitor dispersions based on organosilanes and hydrophobic solvents capable of coagulating on the surface of metals with the formation of polymer-like protective coatings. The physicochemical properties of protective coatings, as well as the possibility of using dispersions as effective inhibitors of steel corrosion in cooling systems and anticorrosive additives in water-borne paint and varnish dispersions, are to be examined using XPS, electrochemical methods and corrosion tests.

2. Materials and Methods

2.1. Materials and Solutions

Low-carbon steel St3 samples were used, the composition of which is presented in Table 1.

Table 1. Chemical composition of low-carbon steel St3, mass %.

| Material | Concentration of Elements | | | | | | | | |
|----------|---------------------------|------|------|-----|-------|------|-----|-----|-----|
| | Fe | C | Si | Mn | P | S | Cr | Ni | Cu |
| St3 | 98.775 | 0.12 | 0.03 | 0.5 | 0.035 | 0.04 | 0.1 | 0.3 | 0.1 |

For the preparation of inhibitor compositions, the following substances were used:

- Organosilane: vinyltrimethoxysilane (VS) $\text{C}_5\text{H}_{12}\text{O}_3\text{Si}$ (WitcoCo);
- Adsorption-type corrosion inhibitor: 1,2,3-benzotriazole (BTA) $\text{C}_6\text{H}_5\text{N}_3$ (GP Chemicals);
- Hydrophobic solvent: trichloromethane CHCl_3 (LenReactiv);
- Surfactant Strodex TH-100 (Strodex). The Strodex base is the sodium salt of an aliphatic ester of phosphonic acid $(\text{R}_1)(\text{R}_2)\text{P}(\text{OONa})$.

2.2. Steel Surface Treatment and Preparation of IDs

Prior to experiments, the steel samples were preliminarily grounded using 1000-grit micron sandpaper (Smirdex, Moscow, Russia) and then washed in an ultrasonic bath, “Sapphire-0.8 TC” (“Sapphire”, Moscow, Russia), in a mixture of ethanol and toluene $\text{C}_2\text{H}_5\text{OH}/\text{C}_7\text{H}_8 = 1:1$ for 15 min.

An electrolyte of the following composition was used as a background aqueous solution: 0.4 M H_3BO_3 + 0.1 M $\text{Na}_2\text{B}_4\text{O}_7$ + 0.01 M NaCl with pH 6.7 [32]. The concentration of BTA and VS in CHCl_3 was 0.1 M (BTA + VS), and the concentration of the Strodex emulsifier (Chemsale, Samara, Russia) in the background solution was 1%.

2.3. Electrochemical Studies

The cover effectiveness of the steel surface induced by IDs can be characterized by the shift in the local depassivation potential ΔE_{pit} in accordance with Equation (1):

$$\Delta E_{\text{pit}} = E_{\text{pit}}^{\text{inhibitor}} - E_{\text{pit}}^{\text{background}} \quad (1)$$

where $E_{\text{pit}}^{\text{inhibitor}}$ and $E_{\text{pit}}^{\text{background}}$ were determined from anodic potentiodynamic curves [12] in a solution with an inhibitor and without one, respectively.

To record the anodic potentiodynamic curves, an IPC PRO–MF potentiostat (“Volta”, Saint Petersburg, Russia) was used, as well as a three-electrode cell with separated electrode spaces. A platinum plate with an area of 1 cm² served as an auxiliary electrode. A saturated silver chloride electrode (SCE) was used as a reference electrode. Steel disc samples with a working area of 0.64 cm², embedded into polyamide to avoid crevice corrosion, served as a working electrode. All potentials are presented relative to a silver chloride reference electrode.

The IDs described in Section 2.2 were added to the background solution in a ratio of 0.01 M of each component: an organosilane, BTA and a mixture of an organosilane and BTA. The concentration of the Strodex emulsifier was 1%. Before recording the polarization curves, the samples were subjected to cathodic pretreatment at $E = -0.85$ V and then kept in the solution for 15 min until the stationary corrosion potential E_{cor} was established. Potentiodynamic curves were recorded at a potential sweep rate of 0.1 mV \times s⁻¹.

To study the metal/protective layer interface, electrochemical impedance spectroscopy (EIS) studies were performed. The measurements were carried out in a three-electrode electrochemical cell at a corrosion potential. To measure the impedance, a Solartron 1286 (Test Equipment Center, Inc., Gainesville, GA, USA) complex consisting of a potentiostat with a frequency response analyzer FRA 1250 (“Volta”, Saint Petersburg, Russia) was used. The signal was acquired at the corrosion potential with a change in the frequency of the alternating current from 60 kHz to 0.1 Hz ($\Delta E = 10$ mV). The calculation of the elements of the equivalent electrical circuit (EES) was carried out using the Zview 2.4a program (Scribner Associates Inc., Southern Pines, NC, USA).

2.4. X-ray Photoelectron Spectroscopy (XPS)

For XPS studies, rectangular steel plates (10 \times 10 \times 1 mm³) were used, which were subjected to the treatment described in Section 2.2 and tested in the investigated electrolytes. Chemical analysis of surface protective layers was carried out on an ESCALAB-5 spectrometer (VG Thermo Scientific Ltd, East Grinstead, Great Britain). An aluminum anode with a power of 200 W was used as an excitation source. The vacuum in the analytical chamber was maintained at 10⁻⁹ Torr. The analyzer pass energy was set at 50 eV. The binding energy of electrons ejected from the inner shells of atoms was adjusted vs. the XPS peak of C1s electrons of surface contaminations, and the binding energy was taken to be 285.0 eV. The distribution of chemical elements over the depth of the samples was obtained by etching with argon ions with energy of 10 keV, a current density of 20 μ A/cm² and a sputtering rate of 2 nm/min.

2.5. Corrosion Tests

2.5.1. Tests at Room Temperature without Stirring the Solution

To quantify the corrosion rate in aqueous solutions, the gravimetric method was used. Dissolution products from the steel surface were removed using a solution of HCl and urotropine C₆H₁₂N₄. Rectangular plates made of St3 40 \times 30 \times 1 mm³ in size were used. The hydrophobic inhibitor compositions described in Section 2.3 were introduced into the background electrolyte: 0.4 M H₃BO₃ + 0.1 M Na₂B₄O₇ + 0.01 M NaCl pH 6.7. The resulting solutions were mixed on a magnetic stirrer for 15 min, after which steel samples were placed in the electrolytes. The samples were kept in aqueous solutions for 30 days at

room temperature. The corrosion inhibition efficiency of coatings $Z\%$ was determined by Formula (2):

$$Z = \frac{V_{cor1} - V_{cor2}}{V_{cor1}} \times 100\% \quad (2)$$

where V_{cor1} , V_{cor2} represent the corrosion rate ($\text{mg}/\text{dm}^2/\text{day}$) in the absence and in the presence of an inhibitor composition, respectively.

2.5.2. Tests at Elevated Temperature and Constant Stirring of the Solution

Corrosion tests of steel samples were carried out in a background 3% NaCl solution, under conditions of constant stirring on a magnetic stirrer at $T = 60\text{ }^\circ\text{C}$ for 12 h. The size of the samples was $40 \times 30 \times 1\text{ mm}^3$. The emulsion VS + BTA + Strodex with an increased concentration of the emulsifier up to 10% was added to the background electrolyte.

2.5.3. Salt Spray Test

Rectangular plates made of St3 $40 \times 30 \times 1\text{ mm}^3$ in size were used. A HomaCryl polyacrylic dispersion (Homa, Moscow, Russia) was used as a water-borne paint coating. Samples of a pure polyacrylic dispersion and an ID of 0.01 M (VS + BTA) + 1% Strodex were investigated. The dispersion was applied to the St3 surface by dipping, after which the samples were dried in air until completely dried. Then, the samples were placed in a Weiss SC/KWT 450 salt fog chamber (Weiss Umwelttechnik, Reiskirchen, Germany) (5 wt% NaCl) at a temperature of $35\text{ }^\circ\text{C}$ and a humidity of 93% for 24 h.

After carrying out corrosion tests, for samples 2.5.2–2.5.3, a quantitative assessment of the proportion of corroded surface St3 was conducted in accordance with the criteria of the ASTM D 610 standard [33].

3. Results

3.1. Electrochemical and Corrosion Studies of IDs in an Aqueous Chloride-Containing Electrolyte

Chronoamperograms were recorded during cathodic pretreatment of $E = -0.85\text{ V}$ (Figure 1a), and potentiodynamic curves (Figure 1b and Table 2) were recorded in the background electrolyte: 0.4 M H_3BO_3 + 0.1 M $\text{Na}_2\text{B}_4\text{O}_7$ + 0.01 M NaCl pH 6.7. The additives used were VS, BTA and Strodex, which is not only an anionic surfactant and active emulsifier but also a corrosion inhibitor. At dispersion formation, the hydrocarbon part of a molecule is within a micelle nucleus, and a negatively charged part—a sodium salt of a phosphonic acid ester—is on the outer side of a micelle nucleus, providing a negative charge to it (Figure 2). Thus, the dispersion particles in electrolytes have a negative charge and are anionic surfactants.

Table 2. Corrosion potential E_{cor} and E_{pit} of steel samples in the background electrolyte with different additives.

| Media | E_{cor} , mV | E_{pit} , mV |
|---------------------------------|----------------|----------------|
| Background solution | −600.0 | −265.0 |
| +1% Strodex | −543.1 | −203.9 |
| +0.01 M VS | −582.3 | −173.7 |
| +0.01 M BTA | −378.6 | −91.8 |
| +0.01 M (VS + BTA) + 1% Strodex | −195.4 | 97.1 |

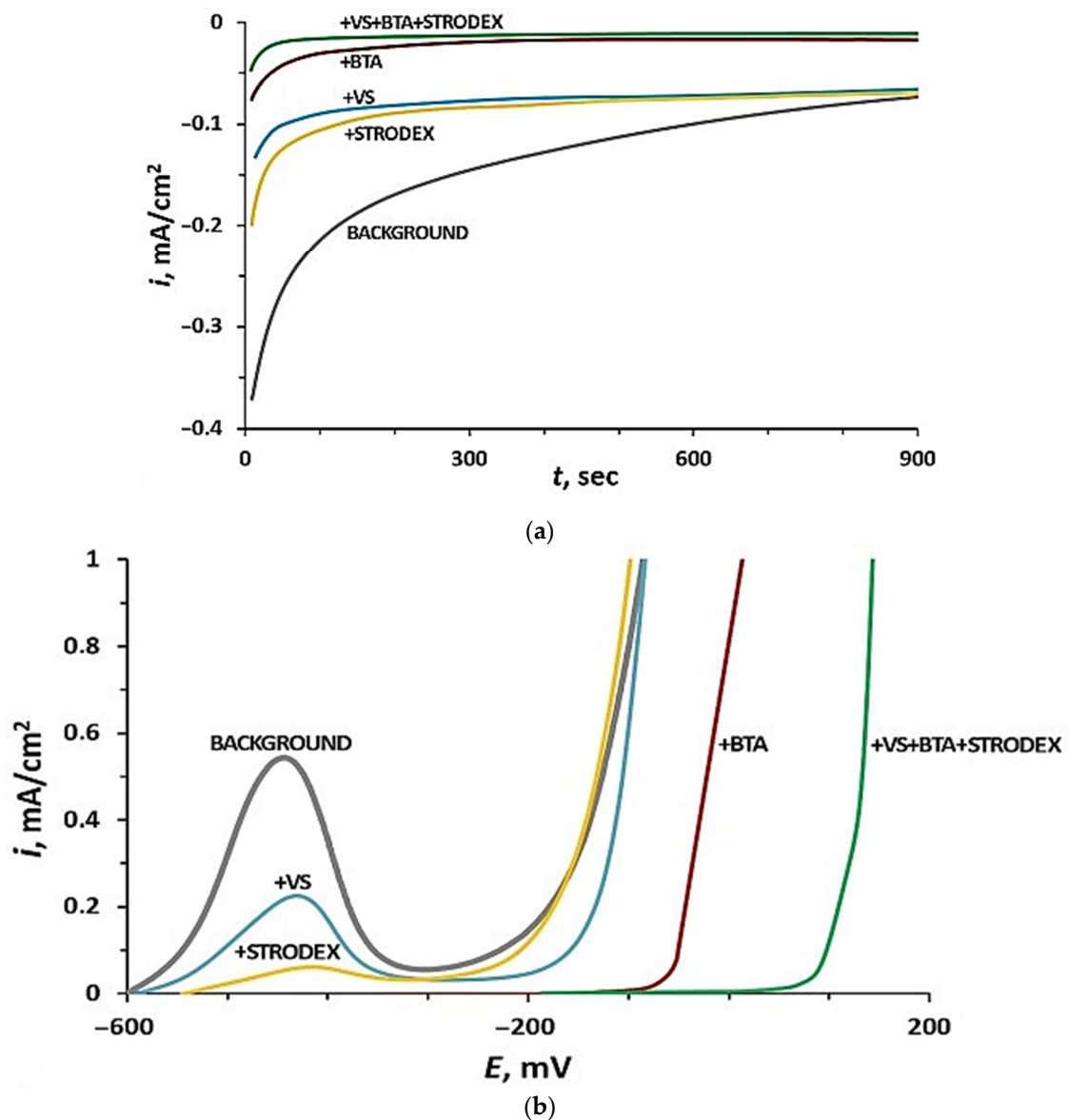


Figure 1. Results of electrochemical studies of St3 in a background solution with the addition of hydrophobic inhibitor dispersions: (a) chronoamperograms; (b) anodic polarization curves.

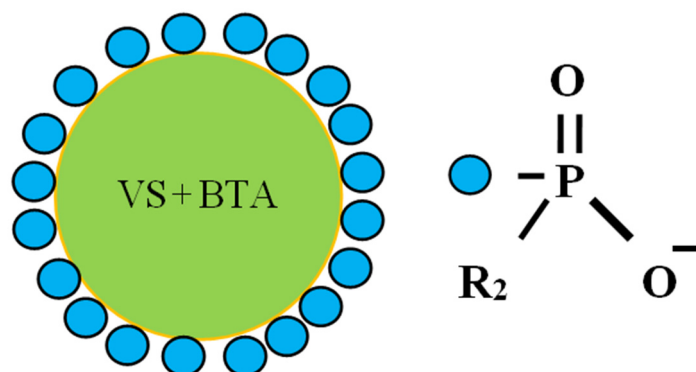


Figure 2. Inhibitor dispersion micelle structure.

From the data presented in Figure 1 and Table 2, it can be seen that in the background solution (0.4 M H₃BO₃ + 0.1 M Na₂B₄O₇ + 0.01 M NaCl pH 6.7), the critical passivation

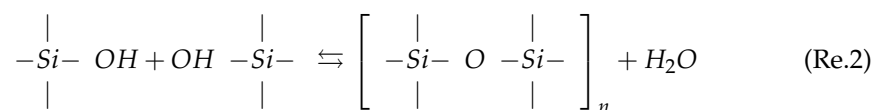
current (peak current) is 0.55 mA/cm^2 , and $E_{\text{cor}} = -600.0 \text{ mV}$. When Strodx and VS are added to the background solution, the peak current decreases by 0.30 and 0.48 mA/cm^2 , and $E_{\text{cor}} = -543.1$ and 582.3 mV , respectively. The addition of VS and Strodx leads to a shift in the pitting potential towards positive values, E_{pit} , $\Delta E_{\text{pit}} = 0.091$ and 0.061 V , respectively. The addition of BTA to the solution passivates the steel ($E_{\text{cor}} = -378.6 \text{ mV}$) and shifts the local depassivation potential (ΔE_{pit}) by 0.173 V . The greatest effect was obtained when steel samples were kept in a mixture of $0.01 \text{ M (VS + BTA) + 1\% Strodx}$. In the presence of this composition, steel was spontaneously passivated, the value of the corrosion potential was -195.4 mV and the pitting potential shifted by 0.362 V .

Along with electrochemical studies, gravimetric corrosion tests of samples in a background solution with the addition of an ID were carried out. Table 3 shows the data of the corrosion tests after 30 days of holding steel samples at room temperature in various solutions.

Table 3. Corrosion rate of steel samples and protective effect in various electrolytes.

| Media | V_{cor} , $\text{mg/dm}^2/\text{day}$ | Corrosion Inhibition Efficiency Z , % |
|--------------------------------|--|---|
| Background solution | 14.2 | – |
| +1% Strodx | 9.6 | 32.4 |
| +0.01 M VS | 8.3 | 41.5 |
| +0.01 M BTA | 6.4 | 54.9 |
| +0.01 M (VS + BTA) + 1% Strodx | 2.1 | 85.2 |

The high protective properties of the inhibitor dispersion $0.01 \text{ M (VS + BTA) + 1\% Strodx}$ are associated with the formation of polymer-like layers on the steel surface during the coagulation of micelles of the dispersion, similar to the way it occurs with the direct introduction of inhibitors into a water solution. The formation of polymer-like structures with the participation of organosilanols involves a series of sequential and parallel stages [12]. At the first stage, the hydrolysis of VS molecules occurs with the formation of silanol $\equiv\text{Si-OH}$ (Reaction (1)), followed by the formation of polyorganosiloxanes (Reaction (2)):



Further, polyorganosiloxanes chemisorb on the surface of metals, and polymer-like film formation is initiated.

3.2. Investigation of the Physical and Chemical Properties of Protective Layers Using EIS

Figure 3 shows the Nyquist and Bode diagrams for steel samples after exposure in an ID of an inhibitor composition at different temperatures with and without stirring. An increase in the radius of the semicircle of the hodograph on the Nyquist plot (Figure 3a) indicates an increase in the protective properties of the coatings. The presence of two maxima in the Bode diagram (Figure 3b) indicates a two-stage process of charge transfer through the coating with two time constants. The first maximum at low frequencies relates to the Faraday impedance, and the second relates to the charge transfer through the protective coating. In this regard, an equivalent impedance circuit was proposed (Figure 4), which was used to calculate the most important parameters of the protective coating.

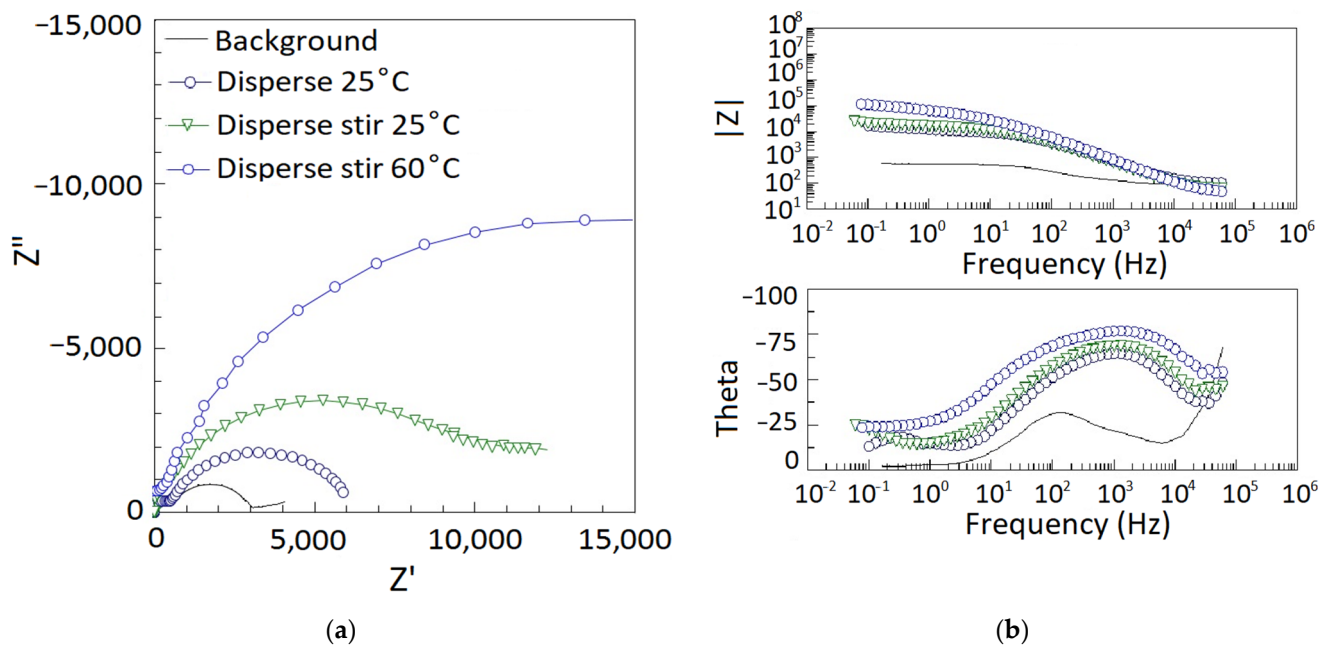


Figure 3. Plots for steel samples after exposure in an ID of an inhibitor composition with and without stirring of the solution for 60 min: (a) Nyquist; (b) Bode.

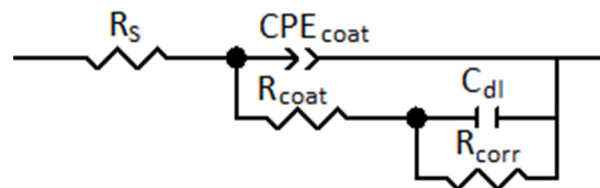


Figure 4. Equivalent circuit for Faraday and electrode impedances, where R_s is the electrolyte resistance, CPE_{coat} is the constant phase element, R_{coat} is the ohmic coating resistance, C_{dl} is the double layer capacity at the metal/coating surface and R_{corr} is the chemical reaction resistance.

Table 4 shows the parameters of elements of the equivalent circuit for different modes of exposure of samples in IDs.

Table 4. Parameters of the equivalent scheme for steel samples after holding them in IDs at various exposure modes.

| Treatment Mode | R_{coat} ($K\Omega \times cm^{-2}$) | R_{corr} ($K\Omega \times cm^{-2}$) | C_{dl} ($\mu F \times cm^{-2}$) | $CPE_{coat-1T}$ ($\Omega^{-1} \times s^n \times cm^{-2}$) | $CPE_{coat-1P}$ |
|-----------------------|--|--|--|--|-----------------|
| Background | 1.1 | 3.1 | 31.4 | 18.7 | 0.94 |
| T = 25 °C | 4.8 | 5.2 | 24.7 | 5.4 | 0.91 |
| Stirring T = 25 °C | 6.3 | 6.7 | 18.2 | 2.1 | 0.87 |
| Stirring T = 60 °C | 8.1 | 7.4 | 9.5 | 0.83 | 0.84 |

It can be seen from the EIS studies that the mixing and temperature rise increase the resistance to charge transfer through the coating and the electric double layer (EDL). A decrease in the capacity of the EDL indicates a reduction in the contact area of the metal with the electrolyte, which also contributes to an increase in the corrosion resistance of the coating. The process of forming a polymer coating with the participation of organosilanes includes several stages, one of which is the transition from gel-like silanols to dense siloxane

structures with the loss of water molecules. This process requires activation energy, and therefore an increase in the temperature promotes the polymerization of the coating and an increase in its corrosion resistance. Stirring stabilizes the dispersion and, by increasing the kinetic energy of micelles, accelerates the disintegration of particles on the metal surface.

A distinctive feature of the formation of polymer films in dispersions is that Reactions (1) and (2) occur in thin layers of the coagulation space in the near-surface space on a metal, the physicochemical properties of which can differ significantly from the bulk properties of a solution during direct inhibition. During the coagulation of micelles, the VS and BTA molecules move from the bulk of the hydrophobic solvent to the metal surface, where they can enter into chemical reactions. The chemical composition and ratio of various forms of organosilanes and BTA affect the processes of polymerization and growth of protective films. In this regard, XPS studies of the surface of the samples were carried out after their exposure to hydrophobic inhibitor dispersions.

3.3. XPS Study

Adsorption of VS and BTA on the Steel Surface from ID

When steel samples are immersed in an aqueous solution of an ID for 10 min, it is possible to determine the chemical state of elements in the chemisorption layer and adjacent outer layers. Figure 5 shows the XPS spectra of $\text{Fe}2p_{3/2}$ at different exposure times of steel samples in IDs.

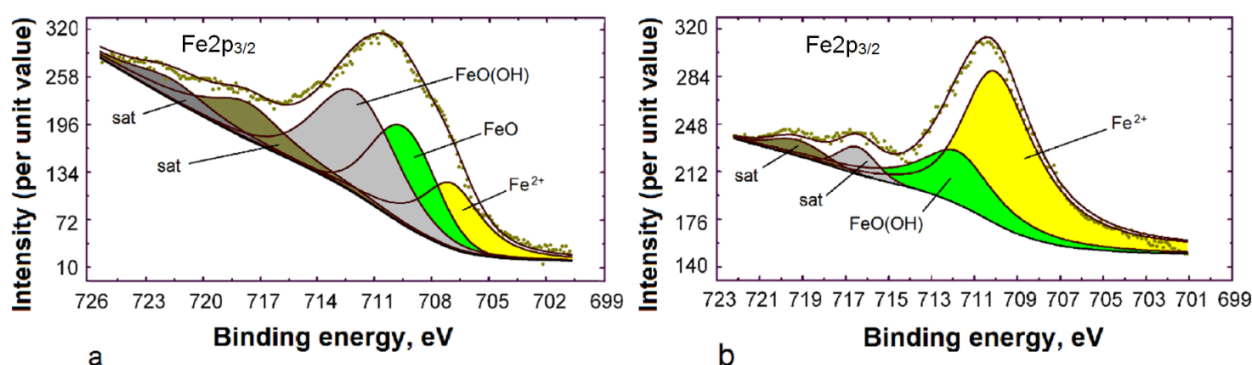


Figure 5. $\text{Fe}2p_{3/2}$ spectra of steel at different exposure times in a hydrophobic inhibitor solution: (a) 10 min; (b) 60 min.

The peak at 707.0 eV corresponds to metallic iron (Figure 5a). Two other peaks with binding energies of 710.2 eV and 712.6 eV belong to an oxide and FeO(OH) , respectively [14]. Thus, the protective layer lies on the hydroxide substrate. According to calculations with XPS MultiQuant software version 7.41 (Dr. Miklós Mohai, Institute of Materials and Environmental Chemistry, Research Centre for Natural Sciences, Budapest, Hungary), the thickness of the protective chemisorbed layer is 2.4 nm. After 60 min of exposure in an ID, an intense peak with energy of 710.2 eV is observed in the spectrum (Figure 5b). Apparently, this peak refers to complex compounds or salts of ferrous iron. Complex compounds can be formed due to Fe^{2+} bridging bonds between NH groups of BTA, acidic Strodx groups and OH groups of VS silanols. The second less intense peak refers to the hydroxide compound of iron.

According to the results of quantitative analysis, organosilanes are the main components of polymer-like coatings. At different stages of the formation of these coatings, organosilanes can exist in two forms: organosilanols and organosiloxanes. Depending on the amount of methoxy groups substituted on OH, two-dimensional or three-dimensional structures can be formed, which, after polycondensation reactions, form polymer-like coatings. Analysis of the $\text{Si}2p$ spectra makes it possible to distinguish between these structures. Figure 6 shows the XPS spectra of $\text{Si}2p$ of silanol and siloxane structures on a steel surface, after immersion of steel samples in an ID for 10 (Figure 6a) and 60 (Figure 6b) min.

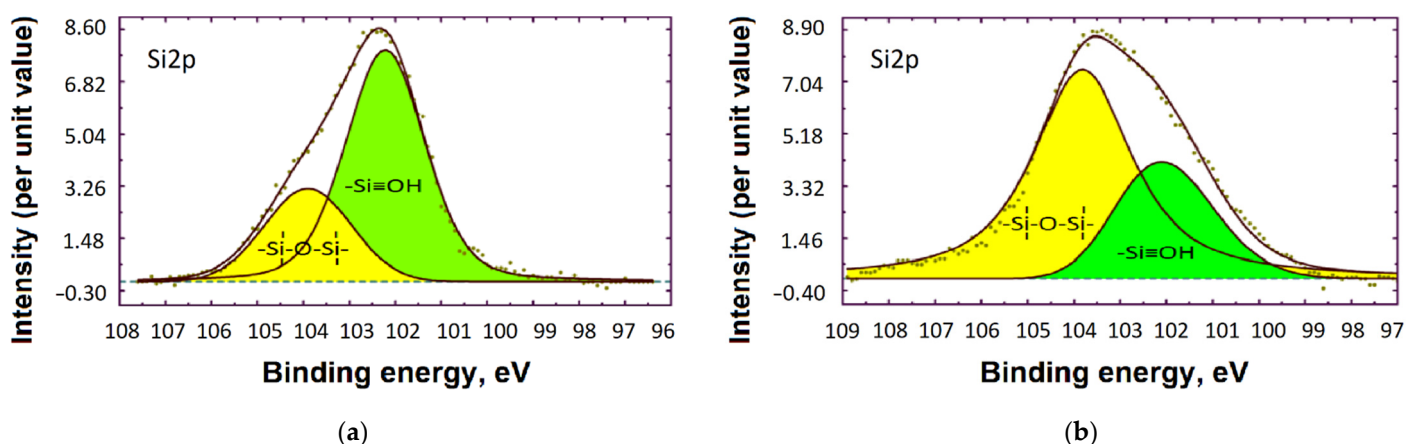


Figure 6. Si2p spectra of samples with various immersion times in a hydrophobic inhibitor solution: (a) 10 min; (b) 60 min.

In the XPS spectrum of Si2p (Figure 6), the peak with $E_b = 102.4$ eV belongs to the silanol groups, and the peak with $E_b = 103.7$ eV belongs to the siloxane groups of VS [12,13]. At the initial stages of formation, the adsorption layer consists mainly of VS silanols. With an increase in the exposure time, the number of siloxane groups increases, which is associated with the polymerization of silanols. The hydrolysis of organosilanes is one of the main stages in the formation of polymer-like coatings. The next stage of polymerization is the reaction of the polycondensation of silanols with each other and BTA.

Analysis of the C1s XPS spectra distinguishes between the individual stages of the polymerization of organosilanes. Figure 7 shows the XPS spectrum of C1s after exposure of the images to the ID.

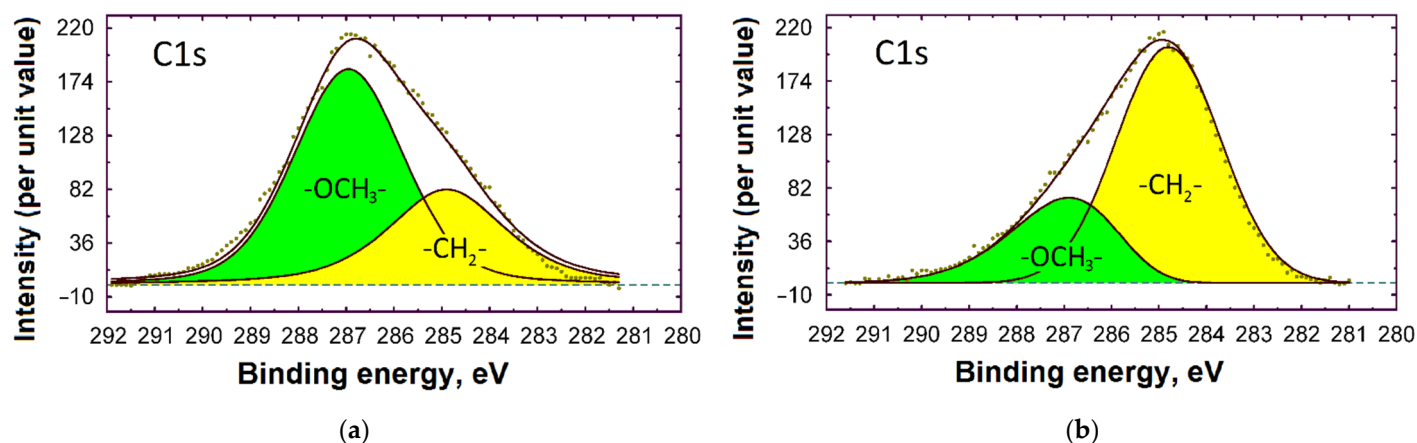


Figure 7. C1s spectra of samples with various immersion times in a hydrophobic inhibitor solution: (a) 10 min; (b) 60 min.

Figure 7b shows that the peak corresponding to the OCH_3 - group decreases in comparison with the same peak in Figure 7a. This indicates that $\approx 70\%$ of the OCH_3 - groups underwent hydrolysis. With complete hydrolysis, the OCH_3 peak disappears altogether.

The nitrogen atoms in the XPS spectra of the samples belong to BTA molecules. According to [12], BTA is a bifunctional additive in inhibitor compositions capable of forming donor–acceptor bonds with iron and entering into condensation reactions with organosilanol. Pyrolic nitrogen atoms participate in the formation of donor–acceptor bonds, and in the reactions of the polycondensation of the NH group of BTA. During chemisorption, the electron density is redistributed on nitrogen atoms, which makes it possible to identify the BTA molecules involved in the formation of chemical bonds with the metal during chemisorption. Figure 8 shows the XPS spectra of N1s after 10 min of exposure in the ID.

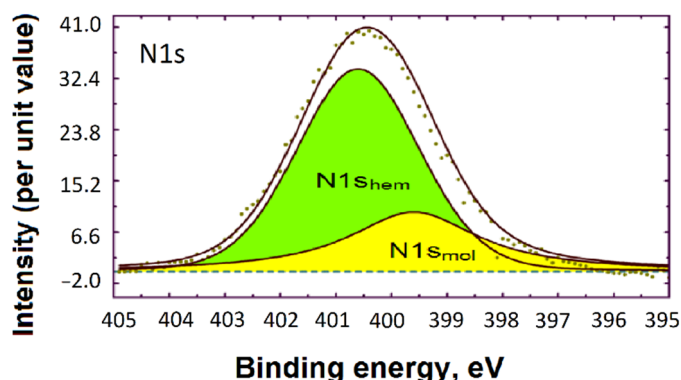


Figure 8. N1s spectrum of BTA adsorbed on steel surface after exposure in ID.

After the decomposition of the N1s spectrum into components, two peaks with energies of 400.6 eV and 399.6 eV can be distinguished, which can be attributed to the inner layer chemisorbed onto the metal and the outer layer of the polymer coating, respectively. With an increase in the coating thickness, only a singlet peak with an energy of 399.6 eV remains on the N1s spectra.

The study of the chemical composition of the surface of steel samples after exposure in the ID showed that it forms a protective layer, the composition of which is shown in Table 5. The thickness of the protective layer was determined using ion etching. After holding in the ID, the samples were washed in running water and in a distilled ultrasonic bath for 15 min.

Table 5. Chemical composition of the protective layer on steel after holding in a dispersion of the composition 3% NaCl + 0.01 M (VS + BTA) + 1% Strodex.

| Exposure Time | Fe | Si | N | O | C | P | Thickness, nm |
|---------------|-----|------|-----|------|------|-----|---------------|
| 10 min | 6.6 | 10.4 | 6.2 | 36.2 | 38.3 | 2.3 | 6 ± 0.5 |
| 60 min | 1.5 | 14.2 | 1.2 | 41.4 | 40.1 | 1.6 | 15 ± 0.5 |

As it follows from the data in Table 5, relatively thick protective layers are formed on the sample, which contain Si, N and P atoms, which are part of the molecules of organosilanes, BTA and Strodex. According to [12,13], these molecules form polymer-like structures on steel as a result of the hydrolysis of organosilanes and the polycondensation reaction with BTA molecules. Strodex molecules, which are derivatives of phosphonic acid, can also undergo polycondensation with organosilanols. Figure 9 shows the distribution of chemical elements over the depth of the protective layer after 60 min of exposure of the samples in the ID.

The protective layer contains siloxane structures (Si), BTA molecules (N) and the Strodex emulsifier (P). Based on the stoichiometry of the molecules, the ratio of BC, BTA and Strodex molecules in the coating after 10 min of exposure (Table 5) is ≈10:2:2. With an increase in the coating thickness, the proportion of organosilanes increases. BTA molecules are located mainly at the border with the metal. The significant thickness of the protective layer should be noted, which remains on the surface of the samples even after they are thoroughly washed in an ultrasonic bath with water for 15 min. The chemical composition, thickness and protective properties of the surface structures indicate that polymer-like films are formed on the steel surface after exposure to the ID containing VS and BTA, similar to the films obtained with the direct introduction of these inhibitors. With the correct selection of a hydrophobic solvent and emulsifier, the IDs are very stable and can be used in cooling systems and as inhibitor additives for long-term storage.

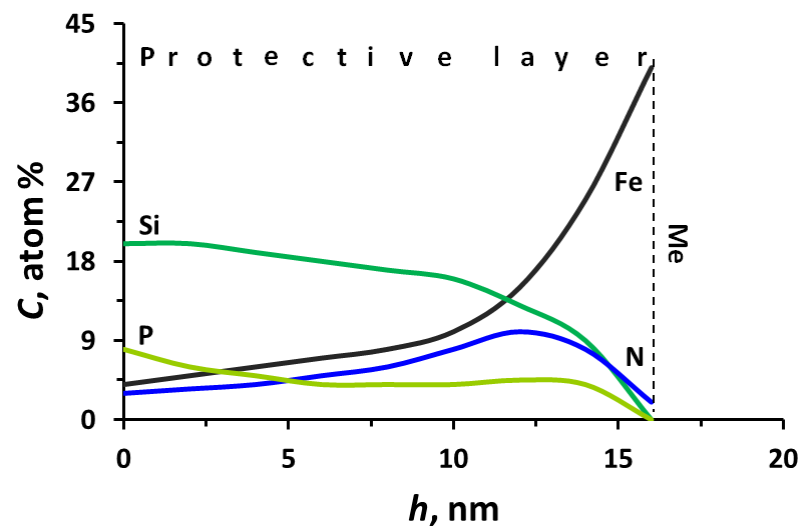


Figure 9. Distribution of the concentration (C) of chemical elements over the depth (h) of the protective layer after 60 min of exposure of the samples in ID and ultrasonic cleaning.

3.4. Corrosion Tests

3.4.1. Tests at Elevated Temperature and Constant Stirring of the Solution

The corrosion tests under conditions of long exposure at room temperature, carried out earlier, show the high efficiency of IDs for protection against uniform and pitting corrosion. It is of interest to investigate the protection of steel samples under conditions of elevated temperature and stirring. Figure 10 shows the surface of the samples after 12 h of testing with constant stirring and a temperature of 60 °C. On steel samples, after holding them in a solution of 3% NaCl, extensive areas of corrosion were observed (Figure 10a and Table 6).

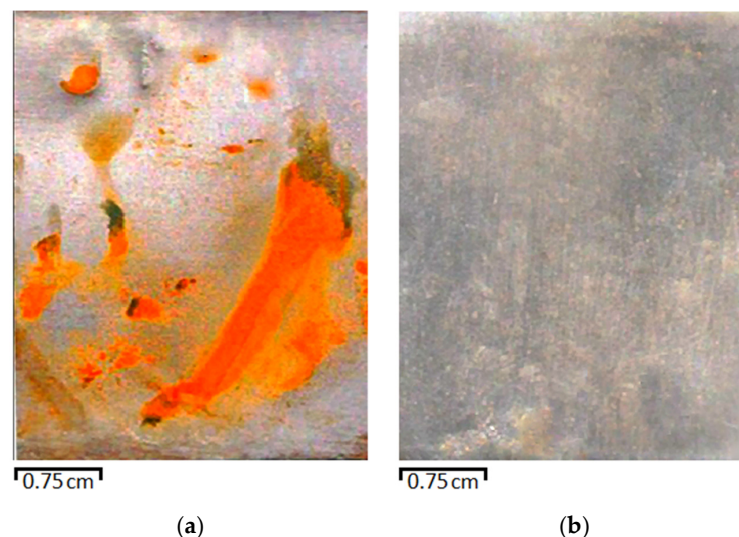


Figure 10. Appearance of steel samples after 12 h of exposure in 3% NaCl solution with and without ID addition at constant stirring at $T = 60$ °C: (a) 3% NaCl; (b) 3% NaCl + 0.01M (VS + BTA) + 1% Strodex.

The addition of 0.01 M (VS + BTA) + 1% Strodex leads to significant inhibition of corrosion of the steel samples (Figure 10b and Table 6). Stirring stabilizes the dispersion, which improves the corrosion protection of the steel. An increase in the exposure time (t) can reduce the protective ability and stability of the dispersion due to the coagulation of micelles in the volume of the electrolyte and emulsion stratification. However, the

polymerization of silanols on the metal surface becomes easier with increasing t ; therefore, the temperature conditions must be specially selected for such IDs.

Table 6. The proportion of corroded steel surfaces after 12 h of exposure to 3% NaCl solution at $T = 60\text{ }^{\circ}\text{C}$ and constant stirring of the solution.

| Solution | Corrosion Damage Rate, % |
|--|--------------------------|
| 3% NaCl | 37 |
| 3% NaCl + 0.01 M (VS + BTA) + 1% Strodex | 3 |

3.4.2. Tests under Conditions of Anodic Polarization

The obvious advantages of using inhibitor compositions based on silanes in the form of dispersions to protect metals from corrosion largely depend on the choice of surface-active additives, which should not only be effective emulsifiers but should also have the ability to impart a positive or negative charge to micelles. The negative electric charge on the molecules or particles of the dispersion promotes adsorption and the formation of stronger bonds between them and the anodic areas of the metal surface or the anodes of galvanic pairs (cooling systems with different metals). Another application of dispersions of organosilanes having a negative charge on micelles is their use in the application of anticorrosive coatings using electrophoresis. Not only the micelles of the dispersion but also the ions of the sodium salt of a phosphonic acid ester have a negative charge, which are formed after the dissociation of the Strodex molecules. In this regard, during anodic polarization, not only the decomposition products of micelles but also the emulsifier molecules will be deposited on the samples.

Figure 11 shows the surface of the samples after anodic polarization in aqueous solutions and dispersions. The appearance of the sediment (Figure 11a) indicates that inhibition of individual parts of the surface occurs, since the coating is not continuous and is located on the surface in the form of islands. During anodic deposition from dispersions, a full polymerization of organosilanes occurs, and a continuous film with high protective properties is formed (Figure 11b).

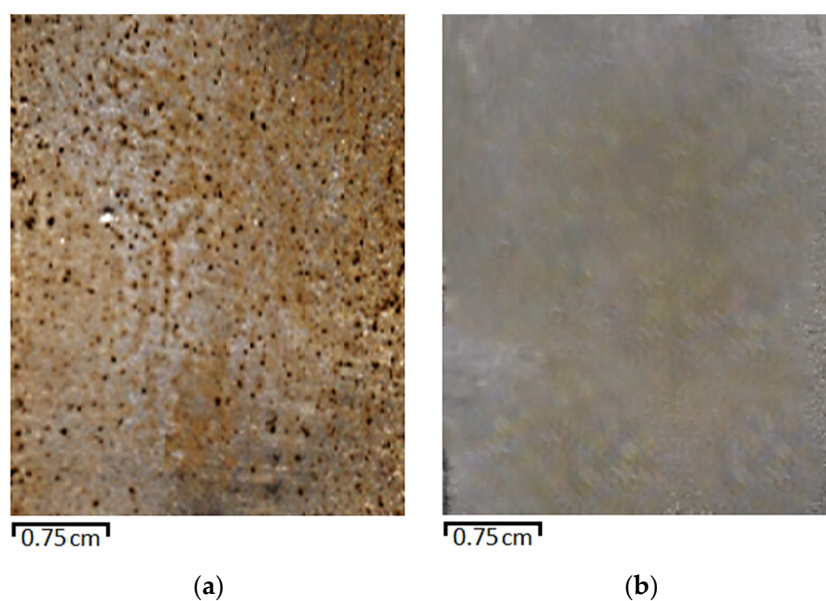


Figure 11. Appearance of the surface of steel samples subjected to corrosion tests under various conditions: (a) anodic polarization for 10 min at $i = 20\text{ mA/cm}^2$ in 3% NaCl solution + 0.01 M (VS + BTA); (b) anodic polarization in ID 0.01 M (VS + BTA) for 10 min at $i = 20\text{ mA/cm}^2$ in 3% NaCl solution + 1% Strodex.

3.4.3. Paint Coatings Salt Spray Test

One of the promising areas of application of organosilane dispersions is the inhibition of water dispersion paints and varnishes (WD paintwork materials). Polyacrylic dispersion is the basis of many high-quality paintwork materials. The addition of an ID to the HomaCryl polyacrylic dispersion significantly increases the anticorrosive properties of the resulting coating. Figure 12 and Table 7 show the test results of steel samples modified in a pure polyacrylic dispersion of HomaCryl and with the addition of 0.01 M (VS + BTA) + 1% Strodex, after 24 h exposure in a salt fog chamber.

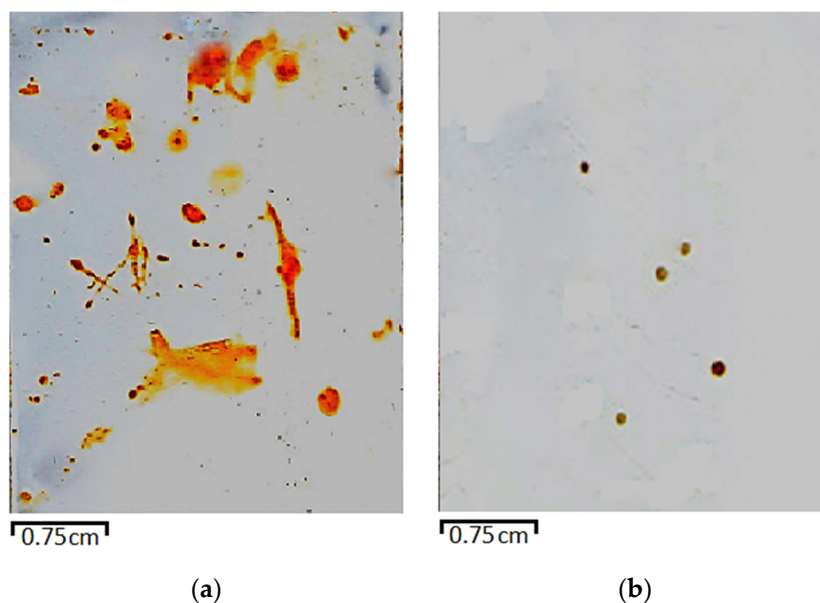


Figure 12. Appearance of the surface of steel samples after testing in a salt spray chamber for 24 h: (a) Clean HomaCryl coating; (b) HomaCryl + 0.01 M (VS + BTA) + 1% Strodex.

Table 7. Percentage of corroded surface of steel samples with paint and varnish coatings.

| Sample | Test Conditions | Corrosion Damage Rate, % |
|---|----------------------|--------------------------|
| HomaCryl | 24 h salt spray test | 16 |
| HomaCryl + 0.01 M (VS + BTA) + 1% Strodex | | 0.1 |

On the surface of samples with a pure polyacrylic dispersion of HomaCryl, corrosion spots in the form of rust spots are observed (Figure 12a and Table 7), while on the inhibited coating, the amount and nature of damage are significantly different (Figure 12b and Table 7). Microanalysis of the chemical composition of the dark spots, performed using XPS, showed that the defects mainly consist of complexes of the sodium salt of aliphatic ether phosphate (surfactant) with iron. These inclusions appear on the surface of the samples immediately after coating and change little during corrosion tests.

4. Discussion of Results

This study expands the understanding of the use of organosilanes for obtaining protective coatings on steel. A significant disadvantage of solutions with the direct introduction of organosilanes is their low stability due to hydrolysis and rapid polymerization of silanols. This circumstance does not allow the use of organosilanes in systems with a long inhibition time of containers and in cooling systems.

In this regard, there is a need to develop techniques to isolate organosilane molecules from the aqueous medium and, at the same time, preserve their chemical activity with respect to metals. Such technologies are successfully implemented in practice in the paint

and varnish industry when using dispersions of organic film-forming compounds in water-borne paints, by adding emulsifiers to the paint. The difference between the proposed method and the existing ones is that the compositions of film-forming substances in water-borne paints are designed for air polymerization, while in our case, polymerization occurs on the surface of metals in aqueous solutions.

In our work, one of the tasks was to select a hydrophobic substance in which organosilane and a corrosion inhibitor can be dissolved without destroying their molecular structures. For these purposes, benzene, which is compatible with VS and BTA, is well suited [34,35]. An important factor influencing the stability of the dispersion is the choice of the emulsifier. One of the most effective and affordable surfactants is Strodex TH-100. The basis of this emulsifier is the sodium salt of a phosphonic acid ester. In a hydrophobic solvent, the hydrocarbon part of this molecule is part of the micelle core, and the negative charge of the anion of the phosphonic acid ester is located on the outer side of the micelle. The negative charge of the micelle explains the increased adsorption activity of the dispersion at the anodic regions of the metal surface. When the electrode potential is shifted to the anodic or cathodic side, the pH in the near-electrode region changes, and the polymerization process is accelerated due to alkaline or acid catalysis.

The second important factor in the acceleration of polymerization is an increase in the concentration of reactants as a result of the transfer of charged particles to the surface of metals. The studies carried out in this work have shown that during the anodic polarization of steel in dispersion, polymer-like protective layers are formed much faster than in ordinary aqueous solutions. The polymerization of organosilanes in aqueous solutions has been fairly well studied and is most fully described in [2–4,6,11]. According to modern concepts, after hydrolysis and polycondensation in aqueous solutions, gel-like silanol-siloxane structures of a linear or cyclic structure, $\text{HO}[-\text{SiR}_2\text{O}-]_n\text{H}$, are formed. In the course of polymerization, the number of silanol groups decreases, and the number of siloxane groups increases, while the polymer structure becomes denser, and water molecules are lost. We observed such transformations here and in earlier published works [12,13] on the XPS spectra of Si2p. Analysis of the structure of the XPS spectra of Si2p showed that anodic polymerization promotes an increase in the siloxane groups of atoms in the polymer coating. The introduction of other organosilanes with copolymers into the micelle composition can change the direction of movement of ions and the mechanisms of polymerization processes.

5. Conclusions

The use of a hydrophobic solvent promotes the isolation of VS and BTA molecules from the aqueous medium, which prevents the polymerization of these components in the volume of the inhibited solution. Stabilization of the emulsion is provided by the highly effective emulsifier Strodex TH-100, which is also an anionic corrosion inhibitor for low-carbon steels. Such IDs, which contain cyclic azoles, can be used as polymer-type corrosion inhibitors for low-carbon steel. The addition of inhibitor dispersions to the HomaCryl polyacrylic dispersion significantly increases the corrosion resistance of the water-borne paintwork. The coagulation of micelles of the ID and the formation of a polymer-like coating on the surface of steels are accelerated by anodic polarization.

Author Contributions: Conceptualization, project administration, funding acquisition: Y.M.; writing—original draft preparation, writing—review and editing, visualization, supervision: N.G.; methodology, software, validation: I.A.; formal analysis, investigation, resources, data curation: Y.K. All authors have read and agreed to the published version of the manuscript.

Funding: This research was carried out within the state assignment of the Ministry of Science and Higher Education of the Russian Federation (theme No. AAA-A18-118121090043-0 and AAAA-A20-120012390029-7).

Data Availability Statement: Not applicable.

Conflicts of Interest: The authors declare no conflict of interest.

References

1. Petrunin, M.A.; Maksaeva, L.B.; Yurasova, T.A.; Terekhova, E.V.; Maleeva, M.A.; Kotenev, V.A.; Kablov, E.N.; Tsivadze, A.Y. Formation of organosilicon self-organizing nanolayer on an iron surface from vapor phase and their effect on corrosion behavior of metal. *J. Prot. Met. Phys. Chem. Surf.* **2015**, *51*, 1010–1017. [[CrossRef](#)]
2. Semiletov, A.M.; Chirkunov, A.A.; Kuznetsov, Y.I.; Andreeva, N.P. Passivation of steel with aqueous solutions of trialkoxysilanes. *J. Prot. Met. Phys. Chem. Surf.* **2015**, *51*, 1154–1159.
3. Aramaki, K. Protection of iron corrosion by ultrathin two-dimensional polymer films of an alkanethiol monolayer modified with alkylthioxysilanes. *Corros. Sci.* **1999**, *41*, 1715–1730. [[CrossRef](#)]
4. Aramaki, K. Prevention of iron corrosion at scratched surfaces in NaCl solutions by thin organosiloxane polymer films containing octylthiopropionate. *Corros. Sci.* **2000**, *42*, 2023–2036. [[CrossRef](#)]
5. Maleeva, M.A.; Ignatenko, V.E.; Shapagin, A.V.; Sherbina, A.A.; Maksaeva, L.B.; Marshakov, A.I.; Petrunin, M.A. Modification of bituminous coatings to prevent stress corrosion cracking of carbon steel. *Int. J. Corros. Scale Inhib.* **2015**, *4*, 226–234. [[CrossRef](#)]
6. Zhu, D.; Van Ooij, W.J. Corrosion protection of metals by water-based silane mixtures of bis-[trimethoxysilylpropyl]amine and vinyltriacetoxysilane. *J. Prog. Org. Coat.* **2004**, *49*, 42–53. [[CrossRef](#)]
7. Palanivel, V.; Zhu, D.G.; Van Ooij, W.J. Nanoparticle-filled silane films as chromatereplacements for aluminum alloys. *J. Prog. Org. Coat.* **2003**, *47*, 384–392. [[CrossRef](#)]
8. Petrunin, M.A.; Maksaeva, L.B.; Yurasova, T.A.; Terekhova, E.V.; Maleeva, M.A.; Shcherbina, A.A.; Kotenev, V.A.; Kablov, E.N.; Tsivadze, A.Y. The effect of self-organizing vinyl siloxane nanolayer on the corrosion behavior of aluminum in neutral chloride containing solutions. *J. Prot. Met. Phys. Chem. Surf.* **2014**, *50*, 784–791. [[CrossRef](#)]
9. Petrunin, M.A.; Maksaeva, L.B.; Yurasova, T.A.; Terekhova, E.V.; Kotenev, V.A.; Kablov, E.N.; Tsivadze, A.Y. The directional formation and protective effect of self-assembling vinyl siloxane nanolayers on copper surface. *J. Prot. Met. Phys. Chem. Surf.* **2012**, *48*, 656–664. [[CrossRef](#)]
10. Petrunin, M.A.; Maksaeva, L.B.; Marshakov, A.I. The effect of surface siloxane layers on the penetration of hydrogen into iron. *J. Prot. Met.* **2001**, *37*, 139–145.
11. Nazarov, A.P.; Petrunin, M.A.; Mikhailovsky, Y.N. Formation mechanism and anticorrosive properties of thin siloxane films on metal surfaces. *J. Prot. Met.* **1996**, *143*, 251–257.
12. Gladkikh, N.A.; Makarychev, Y.B.; Maleeva, M.A.; Petrunin, M.A.; Maksaeva, L.B.; Rybkina, A.; Marshakov, A.I.; Kuznetsov, Y.I. Synthesis of thin organic layers containing silane coupling agents and azole on the surface of mild steel. Synergism of inhibitors for corrosion protection of underground pipelines. *J. Prog. Org. Coat.* **2019**, *132*, 481–489. [[CrossRef](#)]
13. Gladkikh, N.A.; Makarychev, Y.B.; Chirkunov, A.A.; Shapagin, A.; Petrunin, M.A.; Maksaeva, L.B.; Maleeva, M.A.; Yurasova, T.A.; Marshakov, A.I. Formation of polymer-like anticorrosive films based on organosilanes with benzotriazole, carboxylic and phosphonic acids. Protection of copper and steel against atmospheric corrosion. *J. Prog. Org. Coat.* **2020**, *141*, 105544. [[CrossRef](#)]
14. Kazanskii, L.P.; Selyaninov, I.A. XPS of 1,2,3-benzotriazole nanolayers formed on iron surface. *J. Prot. Met. Phys. Chem. Surf.* **2010**, *46*, 797–804. [[CrossRef](#)]
15. Khadom, A.A. Protection of steel corrosion reaction by benzotriazoles: A historical background. *J. Fail. Anal. Prev.* **2015**, *15*, 794–802. [[CrossRef](#)]
16. Rammelt, U.; Koehler, S.; Reinhard, G. Synergistic effect of benzoate and benzotriazole on passivation of mild steel. *Corros. Sci.* **2008**, *50*, 1659–1663. [[CrossRef](#)]
17. Matheswaran, P.; Ramasamy, A.K. Influence of benzotriazole on corrosion inhibition of mild steel in citric acid medium. *J. Chem.* **2010**, *7*, 1090–1094. [[CrossRef](#)]
18. Solehudin, A. Study of benzotriazole as corrosion inhibitors of carbon steel in chloride solution containing hydrogen sulfide using electrochemical impedance spectroscopy (EIS). *AIP Conf. Proc.* **2014**, *1589*, 164.
19. Finšgar, M.; Petovar, B.; Khanari, K.; Maver, U. The corrosion inhibition of certain azoles on steel in chloride media: Electrochemistry and surface analysis. *Corros. Sci.* **2016**, *111*, 370–381. [[CrossRef](#)]
20. Yao, J.L.; Ren, B.; Huang, Z.F.; Cao, P.G.; Tian, Z. Extending surface Raman spectroscopy to transition metals for practical applications IV. A study on corrosion inhibition of benzotriazole on bare Fe electrodes. *J. Electrochim. Acta* **2003**, *48*, 1263–1271. [[CrossRef](#)]
21. Liu, S.; Xu, N.; Duan, J.; Zeng, Z.; Feng, Z.; Xiao, R. Corrosion inhibition of carbon steel in tetra-n-butylammonium bromide aqueous solution by benzotriazole and Na₃PO₄. *Corros. Sci.* **2009**, *51*, 1356–1363. [[CrossRef](#)]
22. Popova, A.; Christov, M.; Zwetanova, A. Effect of the molecular structure on the inhibitor properties of azoles on mild steel corrosion in 1 M hydrochloric acid. *Corros. Sci.* **2007**, *49*, 2131–2143. [[CrossRef](#)]
23. Silva, D.K.; Ribas, G.C.B.; da Cunha, M.T.; Agostinho, S.M.L.; Rodrigues, P.R.P. Benzotriazole and tolyltriazole as corrosion inhibitors of carbon steel 1008 in sulfuric acid. *Electrochim. Acta* **2006**, *24*, 323–335. [[CrossRef](#)]
24. Satpati, A.K.; Ravindran, P.V. Electrochemical study of the inhibition of corrosion of stainless steel by 1,2,3-benzotriazole in acidic media. *J. Mater. Chem. Phys.* **2008**, *109*, 352–359. [[CrossRef](#)]
25. Gomma, G.K. Corrosion inhibition of steel by benzotriazole in sulphuric acid. *J. Mater. Chem. Phys.* **1998**, *55*, 235–240. [[CrossRef](#)]
26. Eldakar, N.; Nobe, K. Effect of substituted benzotriazoles on the anodic dissolution of iron in H₂SO₄. *J. Corros.* **1981**, *37*, 271–278. [[CrossRef](#)]

27. Eldakar, N.; Nobe, K. Electrochemical and corrosion behavior of iron in presence of substituted benzotriazoles. *J. Corros.* **1977**, *33*, 128–130. [[CrossRef](#)]
28. Chin, R.J.; Altura, D.; Nobe, K. Corrosion inhibition of iron and copper in chloride solutions by benzotriazole. *J. Corros.* **1973**, *29*, 185–187. [[CrossRef](#)]
29. Selvi, S.T.; Raman, V.; Rajendran, N. Corrosion inhibition of mild steel by benzotriazole derivatives in acidic medium. *J. Appl. Electrochem.* **2003**, *33*, 1175–1182. [[CrossRef](#)]
30. Wagner, C.D.; Davis, L.E.; Zeller, M.V.; Taylor, J.A.; Raymond, R.H.; Gale, L.H. Empirical atomic sensitivity factors for quantitative analysis by electron spectroscopy for chemical analysis. *J. Surf. Interface Anal.* **1981**, *3*, 211–225. [[CrossRef](#)]
31. Plueddenmann, E.P. *Silane Coupling Agents*, 2nd ed.; Plenum Press: New York, NY, USA, 1991; pp. 79–152.
32. Rybkina, A.; Gladkikh, N.; Marshakov, A.; Petrunin, M.; Nazarov, A. Effect of sign-alternating cyclic polarisation and hydrogen uptake on the localised corrosion of x70 pipeline steel in near-neutral solutions. *Metals* **2020**, *10*, 245. [[CrossRef](#)]
33. ASTM D 610-08. *Standard Test Method for Evaluating Degree of Rusting on Painted Steel Surfaces*; ASTM International: West Conshohocken, PA, USA, 2019; pp. 1–7.
34. Gladkikh, N.A.; Makarychev, Y.B.; Maleeva, M.A.; Petrunin, M.A.; Maksaeva, L.B.; Marshakov, A.I. Synergistic effect of silanes and azole for enhanced corrosion protection of carbon steel by polymeric coatings. *J. Prog. Org. Coat.* **2020**, *138*, 105386. [[CrossRef](#)]
35. Petrunin, M.; Maksaeva, L.; Gladkikh, N.; Makarychev, Y.; Maleeva, M.; Yurasova, T.; Nazarov, A. Thin benzotriazole films for inhibition of carbon steel corrosion in neutral electrolytes. *Coatings* **2020**, *10*, 362. [[CrossRef](#)]